

# Electrospun Rapamycin-Eluting Polyurethane Fibers for Vascular Grafts

Jingjia Han · Shady Farah · Abraham J. Domb · Peter I. Lelkes

Received: 26 November 2012 / Accepted: 1 March 2013 / Published online: 9 April 2013  
© Springer Science+Business Media New York 2013

## ABSTRACT

**Purpose** To develop rapamycin-eluting electrospun polyurethane (PU) vascular grafts that could effectively suppress local smooth muscle cell (SMC) proliferation.

**Methods** Rapamycin (RM) was incorporated in PU fibers by blend electrospinning using three distinct blending methods. The drug release profiles and the bioavailability of RM-containing PU fibers in the form of fibrous mats and vascular grafts were evaluated up to 77 days *in vitro*.

**Results** RM-contained PU fibers generated by the three distinct blending methods exhibited significantly different fiber diameters (200–500 nm) and distinct RM release kinetics. Young's moduli of the electrospun fibrous mats increased with higher RM contents and decreased with larger fiber diameters. For all blending methods, RM release kinetics was characteristic of a Fickian diffusion for at least 77 days *in vitro*. RM-PU fibers generated via powder blending showed the highest encapsulation efficiency. The RM in grafts made of these fibers remained bioactive and was still able to inhibit smooth muscle cell proliferation after 77 days of continual *in vitro* release.

**Conclusions** Electrospun RM-containing PU fibers can serve as effective drug carriers for the local suppression of SMC proliferation and could be used as RM-eluting scaffolds for vascular grafts.

**KEY WORDS** drug release · electrospinning · rapamycin · restenosis · smooth muscle cell

## ABBREVIATIONS

AB	almarBlue
BSA	bovine serum albumin
DMEM	Dulbecco's Modified of Eagle's Medium
FBS	fetal bovine serum
HFP-I	1, 1, 3, 3, 3-Hexafluoro-2-Propanol
HPLC	high performance liquid chromatography
NS-IP	normal saline-isopropyl alcohol solution
PANi	polyaniline
PBS	phosphate buffered saline
PGE	PLGA-gelatin-elastin
PLGA	poly(lactic-co-glycolic acid)
PTCA	percutaneous transluminal coronary angioplasty
PU	polyurethane
RM	rapamycin
SMC	smooth muscle cell
SPU	segmented polyurethane
TCP	tissue culture polystyrene

## INTRODUCTION

Restenosis remains the major limitation of stent/graft implantation for coronary artery diseases and occurs in 15–60% of patients with coronary lesions (1,2). Upon vascular injury, the

J. Han · P. I. Lelkes  
School of Biomedical Engineering, Science and Health Systems  
Drexel University, Philadelphia, Pennsylvania 19104, USA

S. Farah  
School of Pharmacy, Faculty of Medicine  
The Hebrew University of Jerusalem, Jerusalem 91120, Israel

A. J. Domb (✉)  
School of Pharmacy, Faculty of Medicine  
Center for Nanosciences and Nanotechnology  
Grass Center for Drug Design and Synthesis  
The Hebrew University of Jerusalem, Jerusalem 91120, Israel  
e-mail: avid@ekmd.huji.ac.il

P. I. Lelkes (✉)  
Department of Bioengineering, College of Engineering  
Temple University, Philadelphia, Pennsylvania 19122, USA  
e-mail: pilelkes@temple.edu

endothelial lining is damaged, exposing the sub-intimal matrix that in turn stimulates the adhesion/activation of platelets and leads to the release of various mitogenic and chemotactic growth factors. These growth factors stimulate vascular smooth muscle cells (SMCs) in the vessel media to proliferate and to migrate into the intima resulting in intimal hyperplasia at the site of injury (1–3). To date, one of the most promising techniques to address this problem is the local delivery of antiproliferative agents (2–8). Higher concentrations of locally deployed drugs can effectively and safely inhibit intimal hyperplasia with minimal systemic effects (4–8). As a natural immunosuppressant, rapamycin (RM, sirolimus) can effectively inhibit the proliferation and migration of SMCs and thus avoid intimal hyperplasia (4–7,9).

Electrospinning is an established versatile platform technology in tissue engineering that can also be used to encapsulate compounds in fibrous scaffolds (10). Various model proteins, such as bovine serum albumin (BSA) (11) and peptide growth factors (12,13), have been incorporated into electrospun fibers. These studies also demonstrated controlled release from the fibrous constructs and retention of the bioactivity of the encapsulated compounds. To date, only few studies reported the incorporation and preservation of rapamycin into electrospun structures. For example, Kim *et al.* (14) introduced rapamycin into a poly(L-lactide-co-caprolactone-co-glycolide)/phospholipid solution via blend electrospinning, yet the therapeutic efficacy of these fibers has not been evaluated. Some recent studies showed that the rate of drug release was dependent on the electrospun fiber diameter: the thinner the fibers, the faster the drug release kinetics (15–17). Electrospinning specific polymer blends can yield fibers with diameters that are smaller than the fibers obtained by spinning the individual solutions (8,18,19). For instance, in one of our previous studies, electrospinning of a PLGA-gelatin-elastin (PGE) blend produced fibers ( $380 \pm 79$  nm) that were significantly smaller than pure PLGA fibers ( $778 \pm 202$  nm) made under identical conditions (19).

We previously described a hybrid polyurethane (PU) vascular graft prepared via a combination of spincasting and electrospinning techniques (20). This compliant hybrid graft composed of a luminal layer with aligned micro-grooves and an outer layer made of an electrospun mesh, promoted the longitudinal alignment and elongation of the luminal endothelial monolayer (20). The Young's moduli in the longitudinal direction were similar to those of the native aorta, and the grafts were able to withstand uniaxial strain of up to 300% (20). Other synthetic polymers, such as poly(D, L-lactide-co-glycolide) that are more rigid than natural arteries, inhibit elastin incorporation into the extracellular matrix of engineered vascular grafts, a naturally occurring process during arterial development (21), resulting in graft failure due to compliance mismatch.

To prevent in-graft/stent restenosis, we now aim to incorporate RM into the outer layer of our hybrid PU grafts via blend electrospinning. We hypothesize that the bi-layered design, where the outer electrospun fibrous layer serves as a drug reservoir for controlled release into the *tunica media*, while the inner drug-free spincast layer functions as a barrier to drug release into the *tunica intima*, will effectively provide sustained drug release while preserving the drug's bioactivity, thus leading to the inhibition of SMC proliferation with minimal, if any, impact on endothelialization of the blood contacting luminal surface (7,8).

In this study, we incorporated RM at various dosages into PU fibrous mats/grfts via blend electrospinning using three distinct blending methods. We then examined the effects of RM loading on the fiber morphology, fiber size, the tensile properties of fibrous mats, and the release of RM from PU mats and grafts *in vitro*. The ability of RM-containing PU mats and grafts to inhibit the proliferation of SMCs was also examined *in vitro*. We postulate that our RM-containing PU grafts will serve as a drug reservoir to sustain localized drug release over a prolonged period of time following implantation and that these RM-eluting grafts will significantly delay the onset of intimal hyperplasia and lead to improved graft patency.

## MATERIALS AND METHODS

### Materials

Biospan<sup>®</sup> segmented polyurethane (SPU) was provided by DSM, Biomedical (Berkeley, CA, USA). Rapamycin (RM, Sirolimus, cat no: R-5000) was purchased from LC Laboratories (Woburn, MA, USA). 1, 1, 1, 3, 3, 3-Hexafluoro-2-Propanol (HFP, cat no: H0424) were obtained from TCI America (Portland, OR, USA). Alexa Fluor<sup>®</sup> 488 phalloidin (cat no: A12379) was from Invitrogen (Carlsbad, CA, USA). AlamarBlue<sup>®</sup> (cat no: BUF012B) was from AbD Serotec (a division of MorphoSys, Raleigh, NC, USA). Sodium azide was purchased from MERCK (Darmstadt F. R., Germany). Isopropanol, methanol, and ethanol (all in HPLC grade) were from J. T. Baker (Holland). 0.9% Normal saline was from Teva Pharmaceuticals (Israel).

### Electrospinning

Electrospinning was carried out essentially as previously described (18,20). The RM-SPU blend solutions were prepared via three different blending methods. In brief, SPU was dissolved in HFP at 5% (*w/v*); RM powder was either dissolved in HFP at 5% (*w/v*) or 2% (*w/v*) or directly dissolved in the 5% SPU solution. The details of various solutions prepared for electrospinning are listed in Tables I, II, and

**Table I** Concentration of Rapamycin and SPU in HFP via Method “5%”

RM/SPU mass ratio (% w/w)	Mass in 10 mL HFP (mg)		Solute Concentration (% w/v)			Volume of Solutions (A total of 10 mL)	
	SPU	RM	SPU	RM	Total	5% SPU	5% RM
1	495	5	4.95	0.05	5.00	9.9	0.1
5	475	25	4.75	0.25	5.00	9.5	0.5
10	450	50	4.50	0.50	5.00	9.0	1.0
20	400	100	4.00	1.00	5.00	8.0	2.0

**III:** in order to achieve a relative ratio of RM/SPU ( $w/w$ ) at 1, 5, 10, and 20%, the “5%” or “2%” RM solutions were mixed with 5% SPU solution at various volume ratios (Tables I and II) while in powder method (p), certain amount of RM were added into 5% SPU solution (Table III). The prepared RM-SPU solutions are abbreviated, according to the blending method, as RM2, RM5, and RMp, followed by a relative concentration of RM ( $w/w$ , %). The 5% SPU solution, without RM was used as control and denoted as RM (0%). After overnight stirring, the RM-SPU solutions were loaded into a 5 ml plastic syringe (BD Biosciences) equipped with a blunt 18-gauge needle. The solution-loaded syringes were mounted into a syringe pump (KDS100, KD Scientific Single Syringe Infusion Pump, Fisher), and the flow rate was set at 0.8 mL/h. The needle was connected to the positive output of a high voltage power supply (ES30-0.1P, Gamma High Voltage Research, Inc.) set at 15 kV. The distance between the needle tip and the collector was set at 12 cm.

Depending on the experimental needs, three types of fibrous samples were prepared: a) thin meshes (20–50  $\mu\text{m}$  thick) were electrospun on circular 12 mm glass cover slips (Fisher Scientific Inc.) for analysis of fiber morphology and diameter; b) mats (~200  $\mu\text{m}$ ) were electrospun on a grounded rectangular aluminum plate for mechanical testing, *in vitro* drug release, and the *in vitro* bioactivity studies; c) double-layered grafts were fabricated as previously described (see below) on an aluminum mandrel for *in vitro* drug release and bioactivity studies. For preparations of b and c, the mats/grafts were then either peeled off the plate or released from the mandrel. Samples for bioactivity studies were sterilized with UV for 20 min each on both sides in a laminar flow hood before placing them into the cell culture medium (22).

The fabrication of the bi-layered grafts was essentially carried out as previously described (20). A high-speed rotating drill (Dremel, Model 300) was used as a target in lieu of the rectangular plate to collect the electrospun fibers. Approximately 1 ml of 3% SPU solution was first spincast on a slowly rotating mandrel (50 rpm, 4 mm in diameter, 5 cm in length) under a high-intensity halogen lamp (300 W). Immediately following this process, 1 ml RM-SPU solution was electrospun onto the mandrel while rotating at approximately 17,000 rpm. After hydrating in dd H<sub>2</sub>O for 5 min, RM-SPU grafts were released from the mandrel and dried inside a chemical hood overnight.

### Scanning Electron Microscopy Analysis

Samples before and at various time points after *in vitro* release were sputter-coated with platinum/palladium (Pt/Pd) and then visualized with a scanning electron microscope (SEM, Zeiss Supra 50VP or XL-30 Environmental SEM-FEG), as previously described (22). Average fiber diameters were measured using the SEM-internal dedicated software; average and standard deviation were calculated from ten random measurements per image and from at least three SEM images per specimen. At least three specimens were collected from three independent experiments per sample.

### Mechanical Tensile Test

The tensile properties of electrospun RM-SPU mats were characterized with an Instron System (Model 4442, Norwood, MA, USA) using a routine tensile testing protocol (22). The dimensions of rectangular

**Table II** Concentration of Rapamycin and SPU in HFP via Method “2%”

RM/SPU mass ratio (% w/w)	Mass in 10 mL HFP (mg)		Solute Concentration (% w/v)			Volume of Solutions (A total of 10 mL)	
	SPU	RM	SPU	RM	Total	5% SPU	2% RM
1	487.5	5.0	4.88	0.05	4.93	9.75	0.25
5	442.0	23.2	4.42	0.23	4.65	8.84	1.16
10	391.5	43.4	3.92	0.43	4.35	7.83	2.17
20	307.5	77.0	3.08	0.77	3.85	6.15	3.85

**Table III** Concentration of Rapamycin and SPU in HFP via Method "Powder"

	RM/SPU mass ratio (% w/w)	Mass in 10 mL HFP (mg)		Solute Concentration (% w/v)		
		SPU	RM	SPU	RM	Total
1		500	5	5.00	0.05	5.05
5		500	26	5.00	0.26	5.26
10		500	56	5.00	0.56	5.56
20		500	125	5.00	1.25	6.25

mats (10 mm×5 mm×20–200  $\mu$ m, L×W×H) were measured with a digital caliper (L, W) or with a SEM (H). A 50 N load cell and strain speed of 10 mm/min were used. All tests were designed to stop at a strain of 300%. The Young's modulus was calculated from the slope of the initial linear segment of the stress-strain curve by segmental linear regression.

### In Vitro Measurement of Drug Release

To determine the release pattern of RM incorporated/absorbed SPU mats/grfts, 10% normal saline-isopropyl alcohol solution (NS-IP) was used as the release medium, as previously described (23). The release studies were carried out at 37°C using either 0.5 ml/1 ml of NS-IP per 5 mg/10 mg mat or 1 ml of NS-IP per 10 mg graft. The concentration of released RM was measured with high performance liquid chromatography (HPLC) (24) and normalized to the amount of drug release per mg mat/grft. Briefly, reverse phase HPLC on C18 column with a mobile phase consisting of water-methanol (13:87% *v/v*) was used. An isocratic mode was set at a flow rate of 1 ml/min; UV detection was at a wavelength of 277 nm. For each measurement, 10  $\mu$ l release medium containing the released RM was collected and injected into a HPLC system (Hewlett-Packard - HP 1100 System, Germany). Measurements were carried out at days 1, 2, 3, and 7 and further weekly up to day 77. A calibration curve, generated in parallel in the RM concentration range of 0.05–16  $\mu$ g/ml, was used to calculate the concentration of RM in each sample. After each sampling, the release medium was completely replaced with fresh medium.

### Mass Balance of Drug

To determine the efficiency of RM incorporation into the electrospun SPU fibers by different blending methods, the unreleased drug was extracted from the mat samples and analyzed via HPLC (16). Briefly, 150  $\mu$ l of HFP was used to dissolve each mat sample collected after *in vitro* release in a 15 ml tube followed by vortexing for 1 min. Then 4 ml of absolute ethanol was added into the 15 ml tube followed by a second round of vortexing for another 1 min to form a

white suspension. This suspension was then centrifuged for 15 min at 4,000 rpm. The supernatant was transferred to a new 15 ml tube and evaporated till dryness at 40°C. The extracted drug was dissolved in 1 ml HPLC-grade ethanol, filtered through a 0.22  $\mu$ m filter and injected into a HPLC vial for quantitative analysis.

### In Vitro Bioactivity

#### Cell Culture

Bovine aortic smooth muscle cells (SMCs, passages 6–12) were maintained and passaged in Dulbecco's Modified of Eagle's Medium (DMEM) with 4.5 g/L glucose supplemented with 10% fetal bovine serum (FBS, Hyclone, Logan, UT, USA), 0.5% PenStrep (10,000 I.U./mL penicillin, 10,000  $\mu$ g/mL streptomycin solution, Mediatech Inc., Manassas, VA, USA) under standard culture conditions (37°C, 5% CO<sub>2</sub>), as previously described (22). The culture medium was changed every 3 days.

#### AlamarBlue Assay

To assess the bioactivity of RM-SPU fibrous mats or grfts, the cell number/metabolic activity of SMCs was evaluated using the alamarBlue™ (AB) assay, essentially as previously described (22). Briefly, SMCs were seeded at 5,000 cells/cm<sup>2</sup> onto tissue culture treated polystyrene (TCP) in a 24 well plate or a 96 well plate, depending on the size of the samples tested (see below). Following overnight incubation, supernatants were removed and replaced with 0.5 ml (24 well plate) or 0.2 ml (96 well flat bottom plate) fresh complete medium containing 5% (*v/v*) AB in each well. After a 4-h incubation, triplicate (24 well plate) or duplicate (96 well plate) 100  $\mu$ l aliquots of the AB-containing medium were removed from each well for fluorescence readings at Ex/Em=560/590 nm using a synergy BioTek4 microplate reader. Subsequently, 1 ml or 0.2 ml of fresh complete DMEM was used to replace the remaining AB-containing medium. RM-SPU samples, 10 mg (24 well plate) or 1.6 mg (96 well plate), were UV-sterilized and transferred to each well, floating yet completely submerged in the culture medium. The tissue culture plate was then returned to the



incubator. At day 5, the AB fluorescence on the same cell population was accessed. The fluorescence data were corrected for AB “blank” readings of AB-containing medium in the absence of cells for each time point. The AB fluorescence readings taken after the initial overnight incubation were defined as day 0. The AB readings taken at day 5 were normalized to the readings at day 0 for each sample.

Specifically, we carried out two sets of the alamarBlue assay. In order to examine the dose dependence of RM-eluting PU fibers in inhibiting the SMC proliferation, we first evaluated the cell number/metabolic activity using PU samples containing different concentrations of RM (via powder

blending method), prior to *in vitro* drug release. In the second set, we evaluated RM (20%, *w/w*) samples prepared via three different blending methods following 77 days *in vitro* release, in an effort to assess the post-release related differential inhibitory capabilities of RM-eluting PU fibers. In all these experiments, we examined both mat and graft samples.

#### Fluorescence Microscopy

At day 5, cells used for AB reading as above were fixed in 10% buffered formalin for 30 min at room temperature and permeabilized with 0.25% Triton-X100 (Sigma) in 1X PBS.

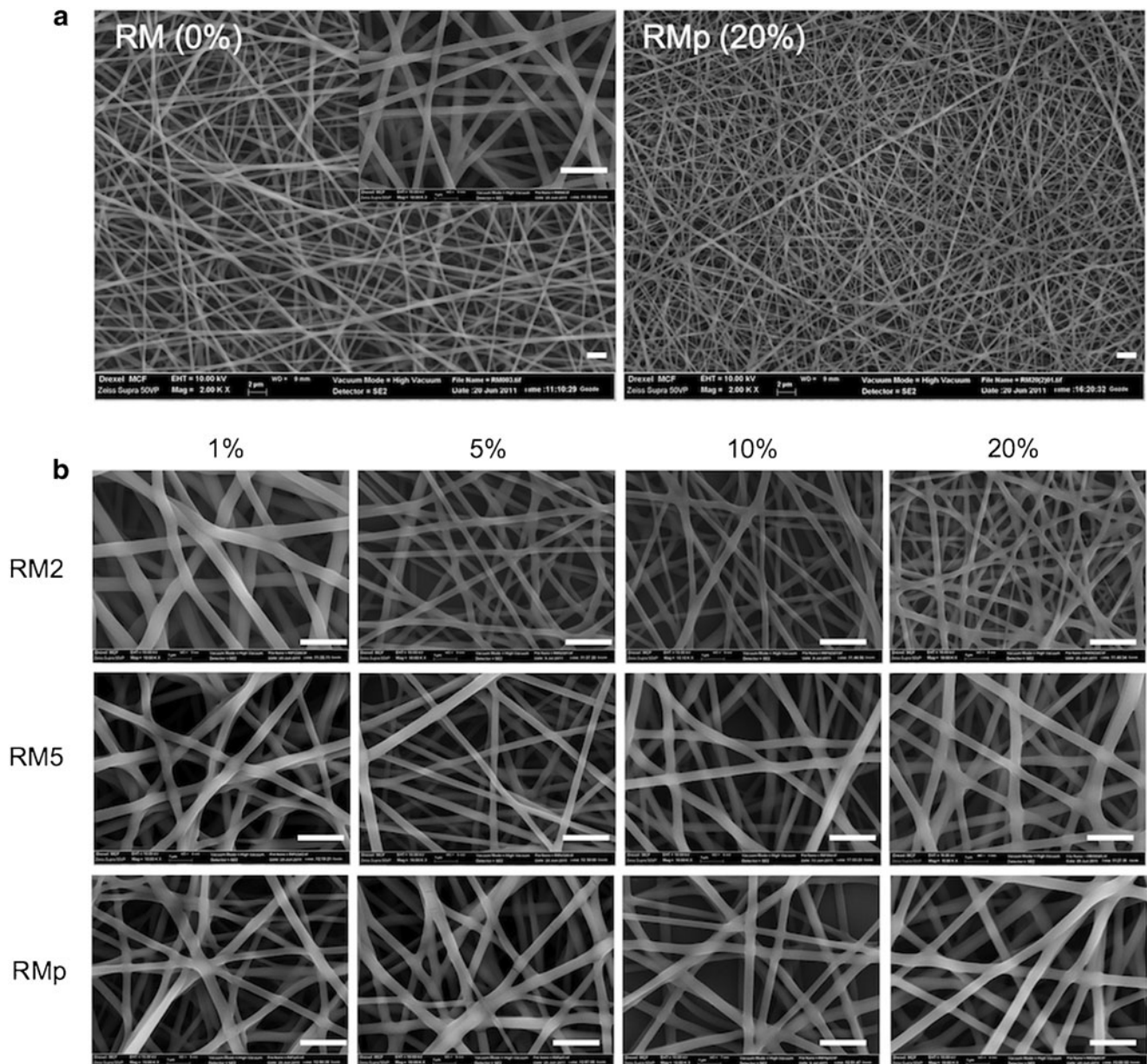


**Fig. 1** SEM images of electrospun RM-PU fibers at a relative RM/SPU ratio (*w/w*) of 0, 1, 5, 10, or 20% via three different blending methods. Scale bar: 2  $\mu$ m.

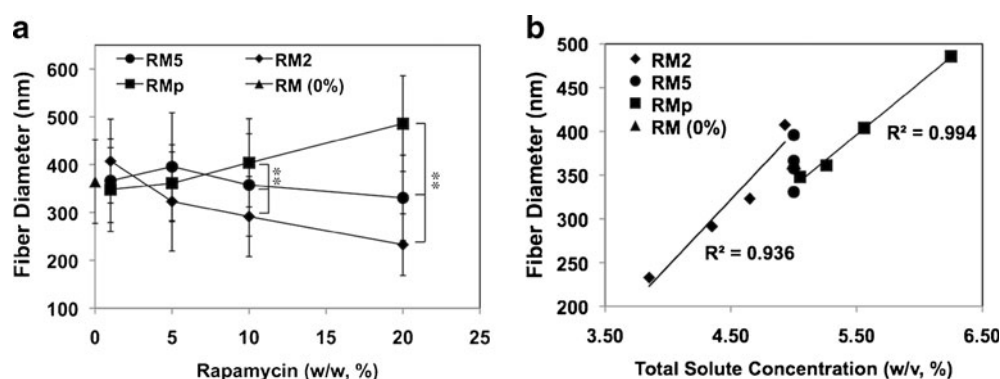


**Fig. 2** (a) Fiber diameter of electrospun RM-PU fibers plotted against the relative concentration of rapamycin (w/w); (b) correlation of fiber diameter with the total solute concentration (w/v) of solutions. Data in (a) are represented as mean  $\pm$  SD ( $n = 90$ ). \*\*:  $p < 0.01$ , by one way ANOVA followed by post hoc Tukey test with all pairwise comparisons. Data in (b) represented the mean.

The samples were then incubated for 15 min with 1  $\mu$ g/mL Hoechst 33258 (Bisbenzimidazole, Sigma) and 1 unit/mL Alexa Fluor<sup>®</sup> 488 phalloidin (Invitrogen), staining nuclei and actin microfilaments, respectively. All constructs were visualized with an inverted Nikon TE 2000U microscope, as previously described (25).

### Statistical Analysis

All the experiments were repeated at least three times in triplicate unless otherwise mentioned. Data are expressed as mean  $\pm$  SD when applicable. Student's *t*-test or ANOVA post hoc Tukey test was used where appropriate. Data were considered to be statistically significant when  $p < 0.05$  and  $p < 0.01$ .

## RESULTS AND DISCUSSION

Percutaneous transluminal coronary angioplasty (PTCA) and bypass grafting are two established therapeutic procedures for

treating coronary artery diseases (9,26,27). Through the use of invasive medical devices, such as catheters, balloons or stents, PTCA removes the plaque and opens the vessels, but will inevitably cause injury to the intimal endothelial layer. Bypass grafting, while detouring the blockage, may also lead to endothelial denudation, platelet adherence and leukocyte infiltration. Eventually, both therapeutic procedures result in the over-proliferation of SMCs and subsequent failure of the stented/grafted vessels (1,8,9). Although drug-eluting stents/grfts have been effective in inhibiting SMC proliferation and improving the vascular patency (1,9), their long-term safety and efficacy remains a challenge, requiring a careful choreography of the combination of polymer, drug and the release kinetics (2). In this study, we employed blend electrospinning to incorporate rapamycin (RM) into electrospun PU fibers via three blending methods for vascular graft application. The RM-eluting PU fibrous mats and grafts were then assessed in terms of their fiber morphology, fiber size, mechanical properties, drug release profiles, as well as their ability to inhibit SMC proliferation *in vitro*.

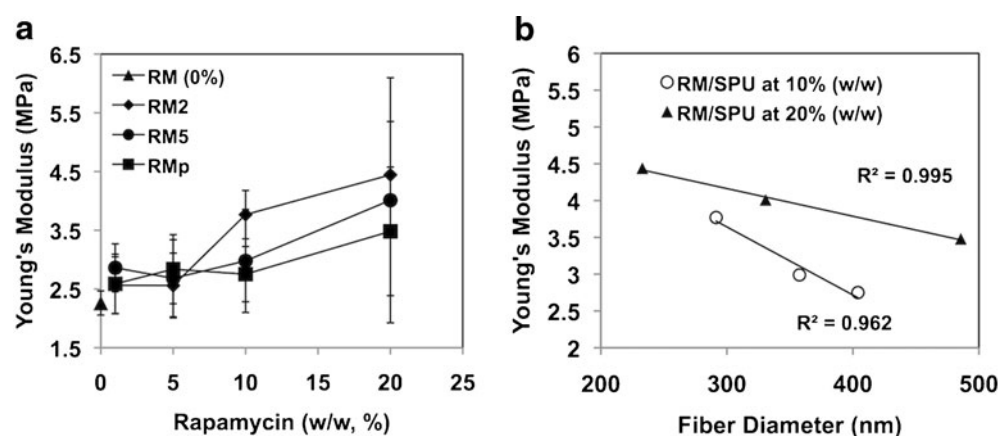


**Fig. 3** (a) Young's modulus of electrospun fibrous mats plotted against the relative concentration of rapamycin (w/w); (b) correlation of Young's modulus of fibrous mats at a relative RM/SPU ratio (w/w) at 10 or 20% with fiber diameter. Data in (a) are represented as mean  $\pm$  SD ( $n = 6$ ). Data in (b) represented the mean.



### Fiber Morphology, Size, and Mechanical Properties

As a strong organic solvent with high polarity (22), HFP completely dissolved both SPU and RM without precipitation after overnight stirring at room temperature. SPU fibers were electrospun from SPU HFP solutions with and without rapamycin, essentially as reported in our previous studies (20,22). As shown in Fig. 1 and detailed in Tables I, II, and III, under the conditions described in Materials and Methods, we were able to electrospin bead-free and uniform electrospun fibers from the various RM-SPU solutions. Little difference in fiber morphology but large variance in the fiber diameter was observed among fibers electrospun from the various solutions (Fig. 1).

By blending RM with SPU via three different methods (Tables I, II, and III), we were able to keep the relative ratio of RM and SPU constant while changing the total solute concentration. For example, at a RM relative weight ratio of 20%, the total solute concentration of solutions prepared via 2%, 5%, and powder blending method were 3.85, 5.00, and 6.25%, respectively. When increasing the RM relative ratio (*w/w*) from 0, 1, 5, 10 to 20%, the fiber diameters of ensuing fiber prepared via 2% blending method were dramatically decreased: all fibers prepared via 5% blending method were

almost identical, and those via powder method were considerably increased (Fig. 2a) with increasing RM contents. Specifically, at 10 and 20% RM (*w/w*), the RM-SPU blend solutions prepared via 2%, 5%, and powder method produced fibers in significantly different size. For example, at 20% RM, where their total solute concentrations are 3.85, 5.00, and 6.25%, the fiber diameters were 233 nm, 331 nm, and 486 nm, respectively (Fig. 2a). Previous studies have reported that the size of electrospun fiber was influenced by various factors, such as solute concentration/solution viscosity (28–30), solution conductivity (29,30), delivery rate of polymer solution (29), and electric field (28,29). The solution conductivity is in general changed by the addition of ionic salts and drugs (29). With the presence of highly charged ions or molecules, the charge density on the surface of ejecting polymer jet is increased, imposing greater thinning and elongation force on the polymer jet therefore resulting in smaller fiber diameters (29). In support of this notion, in one of our previous studies, the addition of a conductive polymer, polyaniline (PANI, 5% *w/w*) reduced the ensuing PANI-gelatin fiber diameters from 800 nm to 60 nm (18). Similar results have also been reported by others, using other binary and tertiary polymer blends (31,32). However, in this study, rapamycin lacks an ionizable group in the pH range of 1–10 (33); its

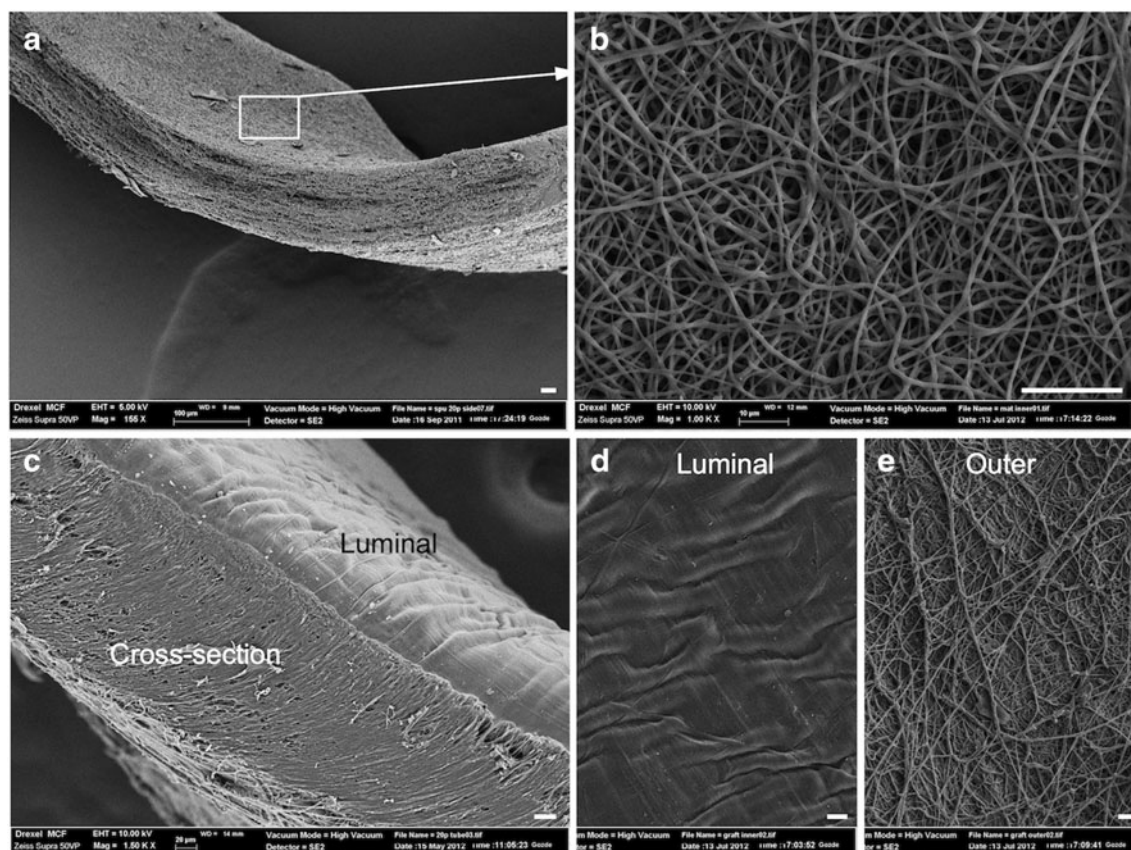


**Fig. 4** SEM images of cross-section (a) and topical view (b) of electrospun mats made of RMp (20%) fibers; cross-section (c), luminal layer (d), and outer layer (e) of bi-layered grafts made of RMp (20%) fibers. Scale bar: 20  $\mu$ m.

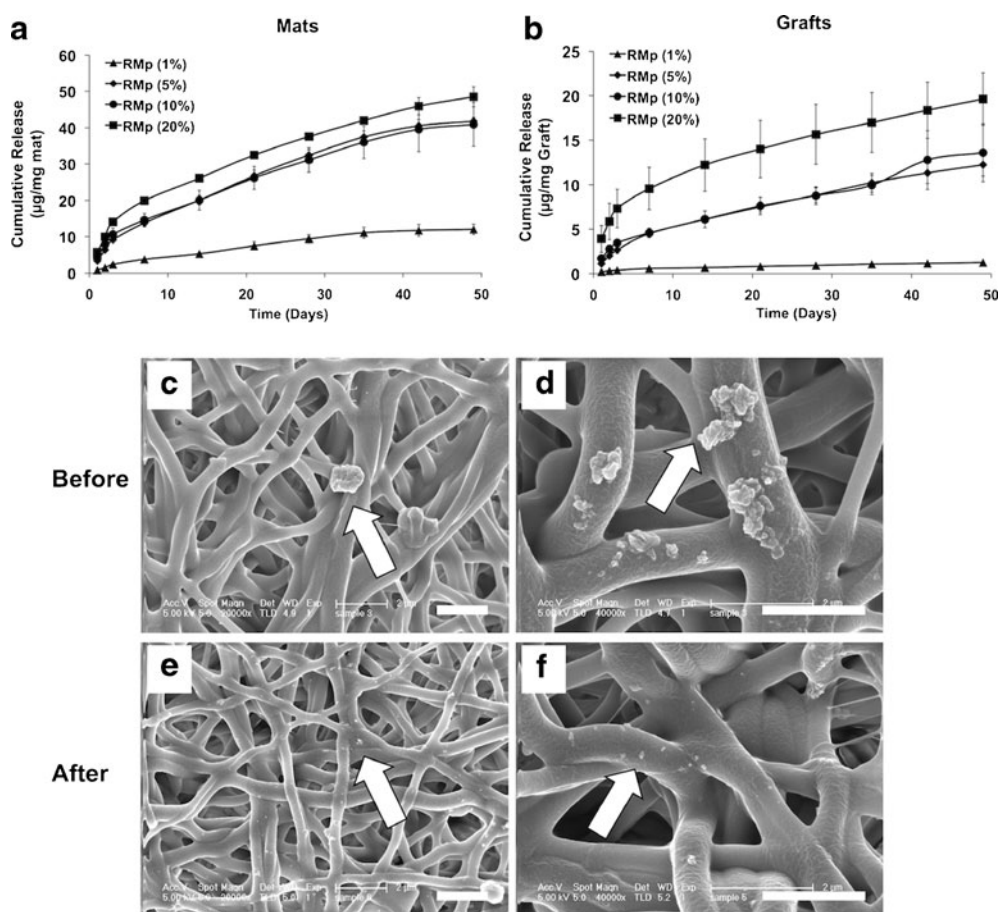


**Fig. 5** *In vitro* drug release profiles of electrospun RMp (1%), RMp (5%), RMp (10%), and RMp (20%) fibrous mats (**a**) and grafts (**b**), and representative SEM images of RMp (20%) fibrous mats before (**c**, **d**) and after (**e**, **f**) release (49 days). Each data point represents mean  $\pm$  SD of three samples. Scale bar: 2  $\mu$ m.

addition to the SPU solution will not affect the blend conductivity. We surmise that our change in the size of the fibers was caused by the altered total solute concentration. To test our assumption, we plotted the diameters of all fibers against their respective total solute concentration. As shown in Fig. 2b, linear positive correlations ( $R^2 > 0.94$ ) were found for samples electrospun via both 2% and powder methods, the solutions of which had varied total solute concentrations. Our observation is consistent with the results reported in the literature, i.e. that the size/diameter of electrospun fibers increases with increased total solute concentration (28–30).

In contrast to the varied effects on fiber diameter, the Young's moduli of the fibrous mats were generally increased with higher relative RM concentration, regardless of the blending methods, indicating that in general, incorporation of RM strengthens the resulting blend fibers (Fig. 3a). This finding is similar to our previous report for PANi-contained gelatin fibers, where the ensuing blend fibrous mats were strengthened with addition of more PANi into the gelatin matrix (18). Interestingly, at a fixed relative RM concentration (10 or 20%, *w/w*), the increase in the total solute

concentration (via blending method 2%, 5%, and powder) yielded a decrease in the average Young's moduli of ensuing fibrous mats (see Fig. 3a, b). Since the relative RM concentrations of these fibers remained constant and their diameters were different (e.g. the fibers of RM2 (20%), RM5 (20%), and RMp (20%)), we surmise that the size of fiber may adversely affect the Young's modulus of ensuing fibrous mats, i.e., fibers with larger diameters, become more elastic. In this context, Tan *et al.* (34) reported that with decreasing diameter, single/individual polycaprolactone fibers were stiffer and less ductile. Our observation on the macroscopic tensile modulus of RM-SPU fibrous mats confirmed and extended these results. By plotting the Young's modulus of fibrous mats against the diameter of corresponding composing fibers (Fig. 3b), we confirmed a negative correlation for samples at a relative RM/SPU ratio of both 10% and 20%. Importantly, the average Young's moduli of RM-SPU fibrous mats at 20% RM (*w/w*) generated by the different blending methods (2%, 5%, and powder) were 4.44 MPa, 4.01 MPa, and 3.48 MPa, respectively, which were comparable to that of natural arteries (Fig. 3) (20).



In order to restrict RM-incorporated SPU fibers to the outer layer of our bi-layered vascular grafts, we first spincast the luminal layer using SPU solutions free of RM and then electrospun blend SPU solutions containing RM to prepare the outer fibrous layer. This specific design was confirmed with SEM: the single-layered electrospun fibrous mat showed a fibrous luminal surface (Fig. 4a, b); in contrast, the bi-layered vascular grafts exhibited a fiber-free, film-like spincast inner layer (Fig. 4c, d) whereas their outer layer showed a fibrous surface (Fig. 4e).

### **In Vitro Drug Release and Bioactivity of RM-SPU Fibers at Various RM Concentrations**

Rapamycin is a hydrophobic, temperature-, pH-, and light-sensitive macrolide antibiotic, and has a relatively long half-life (135 h) in whole human blood (35). The *in vitro* release profile of RM was reported to be largely dependent on the release medium selected (23). In the past, phosphate buffered saline (PBS, with pH 7.4 at 37°C) was employed as a

medium to determine *in vitro* release kinetics. However, although the solubility of RM in aqueous solutions is very low, RM is relatively unstable in the buffer solution such as PBS at pH 7.4, because it hydrolyses, forming new compounds with an opened lactam ring (23,36). In the chromatographic analysis, the new compounds elutes at a lower retention time than RM, leading to the erroneous assessment of the released drug. According to Naseerali *et al.* (23), a mixture of normal saline-isopropyl alcohol (10%, *v/v*, NS-IP) is the most suitable medium for accessing the *in vitro* release kinetics of RM. Therefore, in the present study, we used NS-IP (10%, *v/v*) at 37°C as the aqueous buffer to assess the release kinetics from RM incorporated SPU fibrous mats and grafts.

The RM release study from electrospun RM-SPU mats/grfts prepared via the powder method and with different RM contents was initially carried out over a period of 49 days. All samples exhibited a small initial burst release (<10% of the theoretical total drug loading) within the first 3 days followed by an extended slow release till day 49 (Fig. 5a, b).

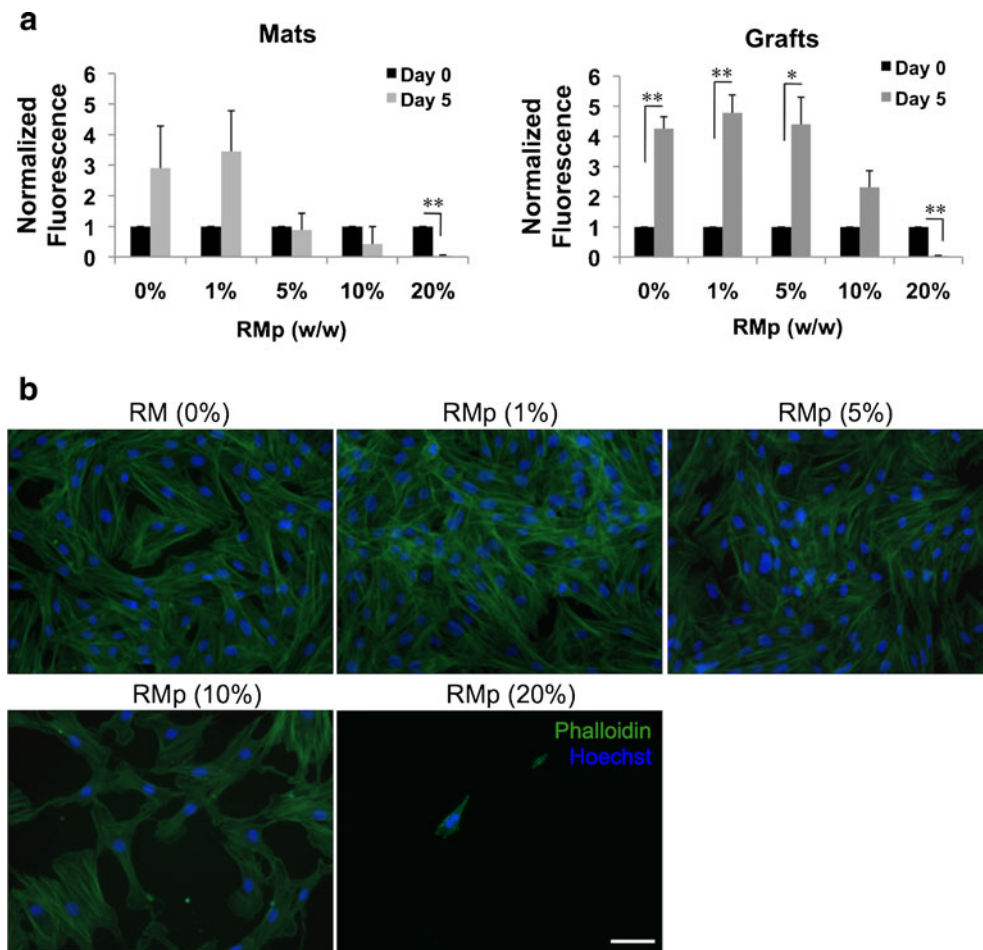


**Fig. 6** (a) AlamarBlue fluorescence of bovine smooth muscle cells (SMCs) cultured in medium containing electrospun fibrous mats or grafts made of RMp fibers at 0, 1, 5, 10, and 20%; (b) Immunostaining images of SMCs cultured in medium containing fibrous grafts manufactured of RMp fibers at 0, 1, 5, 10, 20% at day 5. Staining for nuclei-hoechst (blue) and actin cytoskeleton-phalloidin (green). Scale bar: 100  $\mu$ m. Note: \*:  $p < 0.05$ , \*\*:  $p < 0.01$ , by Student's *t*-test. Data are represented as mean  $\pm$  SD from three independent experiments in triplicates.

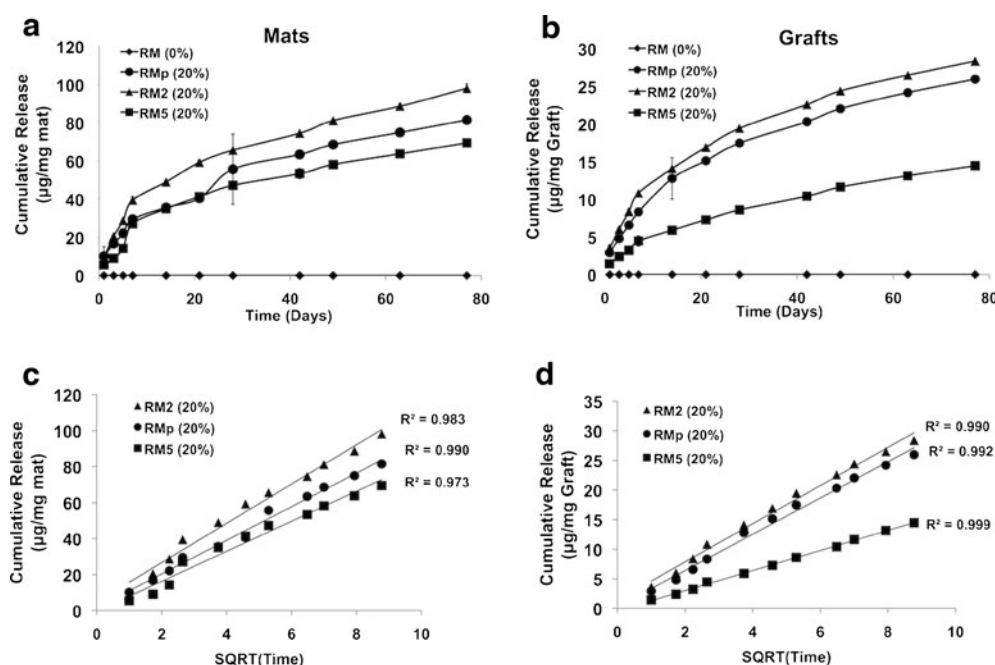


**Fig. 7** *In vitro* drug release profiles of mats (a) and grafts (b) with fibers RM2 (20%), RM5 (20%), or RMp (20%) over 77 days period; data are represented as mean  $\pm$  SD from triplicates. Cumulative RM release plotted against the square root of time for all fibrous mats (c) and grafts (d); data represented the mean from triplicates.

The amount of RM released at each time point was generally dependent on the amount of RM loading, but the release kinetics was not affected by the amount of RM. For mats and grafts comprising fibers containing 20% RM released the maximum drug over the entire period examined. By day 49, these mats/grafts had released approximately 50  $\mu$ g or 20  $\mu$ g RM per mg sample, i.e., 25% or <20% of the theoretical total drug loading, respectively. Notably, the amount of release at each time point was very similar between samples containing RM at 5% and 10%. We surmise that this similarity may be due to our limited initial study period for 49 days and the variances in the encapsulation efficiency (16). Fibers containing 20% RM, occasionally exhibited particle clusters on the surface prior to release (Fig. 5c, d, arrow). After 49-days *in vitro* release, these large particles had mostly disappeared and were replaced with individual particles of significant smaller size (Fig. 5e, f, arrow). The morphology of the fibers after 49 days release was not different

from those before release (Fig. 5c–f). This suggests that RM localized on/near the fiber surfaces accounted for the main sources of drug release within 49 days.

The bioactivity of RM after electrospinning was assessed *in vitro*, based on the effective inhibition of the proliferation of cultured bovine aortic smooth muscle cells (SMCs). For these studies, RM-contained SPU fibrous mats or grafts at different RM concentration (1, 5, 10, 20%, *w/w*) were added to culture wells containing actively growing SMCs. Cell metabolic activity/growth was evaluated biochemically (alamarBlue) and by fluorescence microscopy. Electrospun SPU mats containing fibers with 20% RM were the most effective ones to significantly reduce the number/metabolic activity of SMCs over a 5 day incubation period and thus abrogate their proliferation (Fig. 6a, mats). Similar to electrospun constructs containing 0% RM, mats containing 1% RM showed little inhibitory effect on SMC growth, while those with 5% stalled

**Table IV** Mass Balance of RM20-SPU Mats

Time Point	Sample	Theoretical Loading ( $\mu$ g/mg mat)	Released RM ( $\mu$ g)	Unreleased RM ( $\mu$ g)	Total Mass Balance ( $\mu$ g)	Released RM %	Mass Balance %
Week 7	RM2 (20%)	200	81.096	90.489	171.585	47.26	85.79
	RM5 (20%)	200	56.481	63.180	119.661	47.20	59.83
	RMp (20%)	200	55.646	133.136	188.781	29.48	94.39
Week 11	RM2 (20%)	200	96.334	76.237	172.570	55.82	86.29
	RM5 (20%)	200	65.672	56.825	122.498	53.61	61.25
	RMp (20%)	200	79.447	116.612	196.059	40.52	98.03

cell proliferation leaving the cell numbers at the level found on day 0. Mats containing >10% RM actually “killed” the cells, reducing their numbers to levels below those found at day 0 (Fig. 6a, mats). In contrast, only grafts containing 20% RM significantly inhibited the growth of SMC while those with lower RM concentrations showed no (1%, 5%) or relatively little (10%) inhibitory effect (Fig. 6a, grafts). Immunostaining of cultured SMCs confirmed a reduction in cell number with

increasing RM concentrations similar to that found by alamarBlue (Fig. 6b). In terms of cell morphology, all cells exhibited typical SMC morphology. Specifically, at 10% RM, with more room, the cells exhibited typical SMC spreading; whereas at 20% RM, few if any cells were found remaining in the wells (Fig. 6b). Taken together, the biochemical and microscopic data confirm that grafts containing fibers with 20% RM (*w/w*) can effectively inhibit the proliferation of SMCs during a

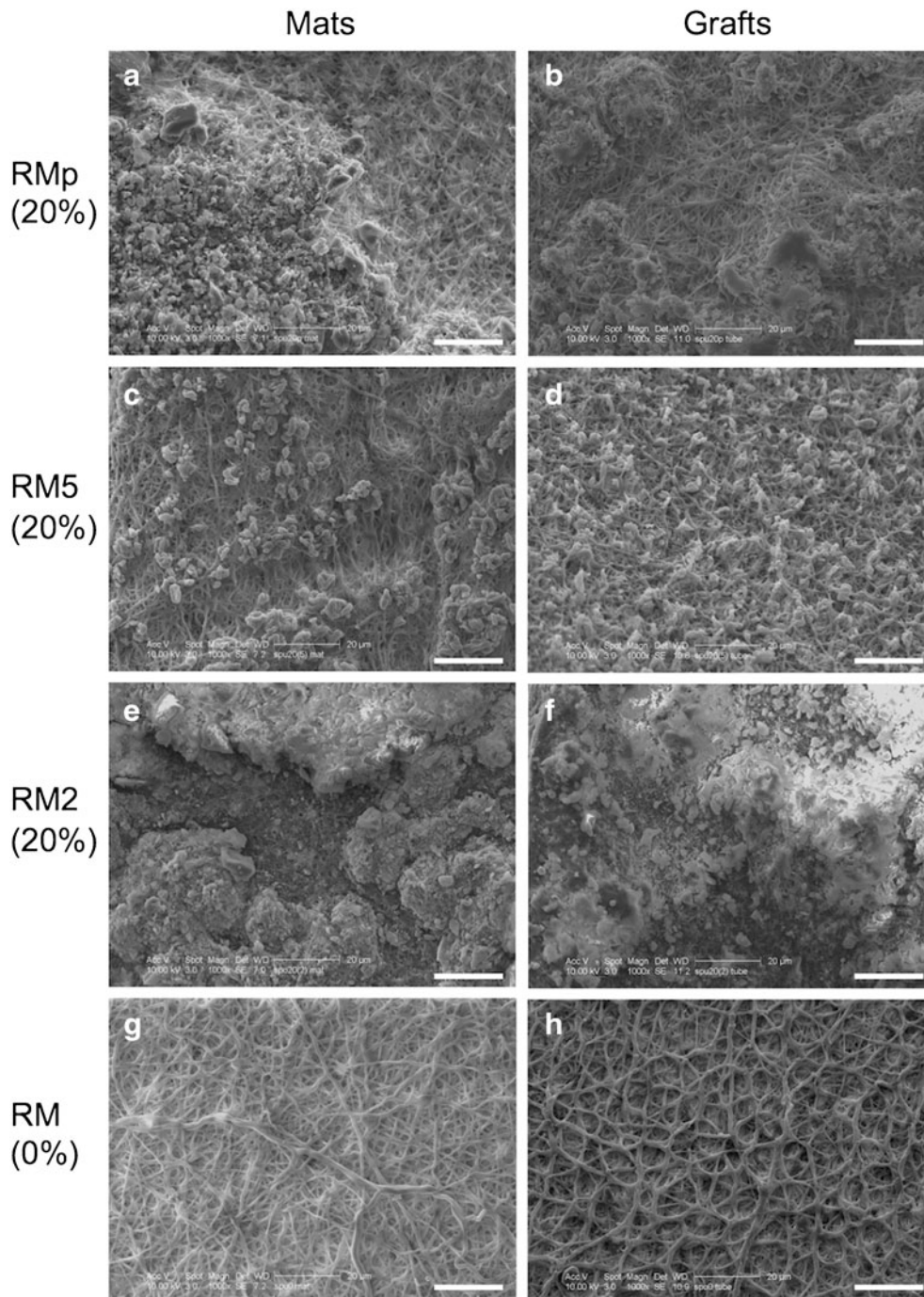


**Fig. 8** SEM images of electrospun mats (**a, c, e, g**) or grafts (**b, d, f, h**) made of RMp (20%) (**a, b**), RM5 (20%) (**c, d**), RM2 (20%) (**e, f**) or RM (0%) (**g, h**) fibers after 77 days *in vitro* release. Scale bar: 20  $\mu$ m.



5-day initial *in vitro* release and our electrospinning process retained at least in part the bioactivity of RM.

### In Vitro Drug Release and Bioactivity of RM20-SPU Fibers via Different Blending Methods

To extend our previous observations for longer periods of time, we prepared electrospun RM-SPU fibrous mats and grafts containing 20% RM with different fiber diameters via the three blending methods as described above, and examined RM release profiles *in vitro* for up to 77 days. All samples exhibited a burst release for the first week followed by a sustained release till day 77. Similar release kinetics was found for all fibers irrespective of the presentation as mats or grafts (Fig. 7a, b). However, the amount of RM release at each time point was different: fibers produced by the 2% method released the highest amount of RM while those manufactured by the 5% method released the lowest. To evaluate the release mechanism, we plotted the cumulative drug release against the square root of time (Fig. 7c, d): the plots for all fibers containing 20% RM were linear ( $R^2 > 0.97$  for the mats,  $R^2 > 0.99$  for the grafts). This suggested the release of RM from all samples till day 77 was controlled by Fickian diffusion, a kinetics that has been widely reported for drug-laden electrospun fibers (8,37–39).

Evaluation of the encapsulation efficiency at weeks 7 and 11, as shown in Table IV, revealed that mats prepared by the powder method displayed the highest incorporation efficiency (>94%), those made by the 5% method exhibited the lowest efficiency (~60%), and samples prepared via the 2% method showed an intermediate efficiency at ~85%. This large variance of incorporation efficiency resulted in a well-informed comparison on the release percentage of RM. At both time points of weeks 7 and 11, cumulative RM released from the RMp mats was the lowest (29.48% at week 7, 40.52% at week 11) while those from mats prepared by the “2%” and “5%” method were close to each other and both were faster than those from RMp mats (Table IV). The negative yet nonlinear correlations between the percentage of RM release and fiber diameter (data not shown), suggests that our data are consistent with the reported fact that the smaller the fiber, the faster the drug release (15–17).

After 77 days *in vitro* release, all SPU fibers containing RM (20%, *w/w*) displayed either clustered particle (RMp (20%) and RM2 (20%)) or particulate surfaces (RM5 (20%)) while those free of RM (RM (0%)) still maintained their smooth fibrous morphology (Fig. 8). Of all samples tested, RMp (20%) fibers displayed an intermediate amount of clustered particles (Fig. 8a, b), while RM5 (20%) fibers showed the least particles, resembling sprouts from fibrous surfaces (Fig. 8c, d). RM2 (20%) fibers exhibited the largest amount of clusters, which covered most of the fibrous surfaces, exposing only few fibers (Fig. 8e, f). It appeared that

our SEM observations correlate well with the drug release data: the higher the amount of RM release, the more (clustered) particles were observed. The cell culture studies of these samples confirmed that samples of RM5 (20%) mats or grafts of RMp (20%) and RM5 (20%) still remained bioactive after a 77-day release and were able to inhibit the proliferation of SMCs (Fig. 9). Of all samples, those prepared by the methods powder and 2% showed a significant difference between mats and grafts (Fig. 9), suggesting that this particular design of our drug-laden grafts allows for sustained RM release and SMC growth inhibition. These bioavailability/bioactivity data correlate generally well with the drug release/SEM data: the higher the amount of released RM during the testing period, the more (clustered) particles, the less bioactive the residual drug laden fibers. Taken together, PU fibers (20% RM, *w/w*) prepared via the powder method might be a suitable choice for generating RM-eluting fibrous vascular grafts because of the favorable combination of high drug encapsulation efficiency, sustained RM release, and well-preserved bioactivity.

In future studies, we plan to evaluate the drug effect, tissue reaction, and patency of our PU grafts (20% RM, *w/w*) prepared via powder method *in vivo*. Innocente *et al.* (40) applied electrospun polycaprolactone (PCL) with slow releasing paclitaxel (PTX) in the abdominal aorta of 18 Sprague-Dawley rats, and showed significant suppression/delay of neointima formation with 100% graft patency for up to 6 months. Mechanically similar to the PCL-PTX grafts and natural arteries (20,40), our PU grafts (RMp (20%, *w/w*)) showed a more sustained drug release profile (with 40% drug

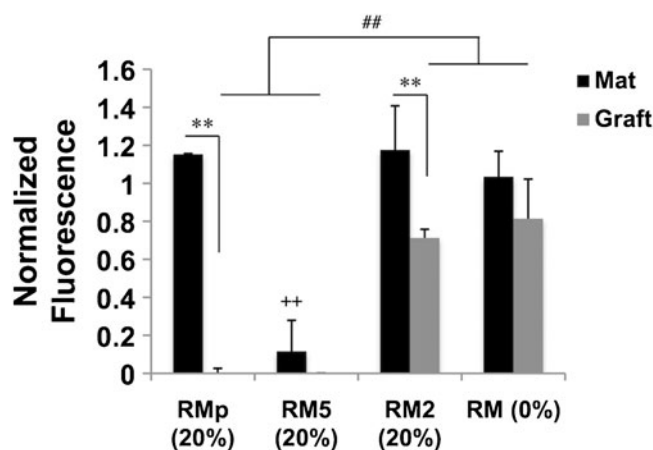


**Fig. 9** Analysis of alamarBlue (AB) fluorescence of bovine aortic smooth muscle cells (BASMCs) cultured in medium containing electrospun RM-SPU mats or grafts after 77 days *in vitro* release. Note: ++:  $p < 0.01$  versus mats of RMp (20%), RM2 (20%), RM (0%), #:  $p < 0.01$ , \*\*:  $p < 0.01$ , by two way ANOVA and post hoc Tukey test with all pairwise comparisons. Data are normalized to the AB fluorescence at day zero and represented as mean  $\pm$  SD.



release in 11 weeks) compared to those found in the PCL-PTX grafts (60% in 4 weeks) *in vitro*. In this context, we envisage that our RM-eluting PU grafts, combined with their unique bi-layered design, may exhibit long-term RM release and bioavailability, resulting in extended graft patency *in vivo*.

## CONCLUSIONS

In this work, we studied the fabrication, release kinetics, and bioactivity of rapamycin-eluting polyurethane fibrous mats and grafts prepared via blend electrospinning. To the best of our knowledge, this study is the first to evaluate of RM bioactivity following electrospinning. Our data demonstrated that electrospinning is a simple and versatile technique to incorporate water-insoluble drugs (such as RM) into polyurethane fibers without (significantly) compromising the morphology and the mechanical properties of the ensuing fibers. In addition, this process allowed continuous Fickian diffusion-controlled RM release for at least 77 days. Electrospinning, via distinct blending methods, yielded RM-PU fibers with different encapsulation efficiency and bioavailability. Grafts made of 20% RM (*w/w*) PU fibers via powder method showed the highest encapsulation efficiency, and maintained bioactive even after 77 days *in vitro* release. We believe that RM-eluting PU fibrous mats and grafts can serve as effective drug reservoirs for the local inhibition of the proliferation of SMCs. We surmise that our bi-layered RM-eluting grafts may be promising candidates for functional vascular grafts with the prospect for long-term safety and patency.

## ACKNOWLEDGEMENTS AND DISCLOSURES

Jingjia Han and Shady Farah equally contributed to this paper. This work was supported by a translational research grant by HUB (DU/BIOMED-IDR/HUJI) from Drexel University and The Hebrew University of Jerusalem. We thank Dr. Gozde Senel-Ayaz (Drexel BIOMED) for her assistance with SEM and Dr. Wahid Khan (IDR) for his assistance with developing the analytical method used to assess drug release.

## REFERENCES

- Liu MW, Roubin GS, King III SB. Restenosis after coronary angioplasty. Potential biologic determinants and role of intimal hyperplasia. *Circulation*. 1989;79:1374–87.
- Fattori R, Piva T. Drug-eluting stents in vascular intervention. *Lancet*. 2003;361:247–9.
- Allaire E, Clowes AW. Endothelial cell injury in cardiovascular surgery: the intimal hyperplastic response. *Ann Thorac Surg*. 1997;63:582–91.
- Stone GW, Moses JW, Ellis SG, Schofer J, Dawkins KD, Morice MC, *et al*. Safety and efficacy of sirolimus- and paclitaxel-eluting coronary stents. *N Engl J Med*. 2007;356:998–1008.
- Kim YH, Park SW, Lee SW, Park DW, Yun SC, Lee CW, *et al*. Sirolimus-eluting stent *versus* paclitaxel-eluting stent for patients with long coronary artery disease. *Circulation*. 2006;114:2148–53.
- Adelman SJ. Sirolimus and its analogs and its effects on vascular diseases. *Curr Pharm Des*. 2010;16:4002–11.
- Wang X, Venkatraman SS, Boey FY, Loo JS, Tan LP. Controlled release of sirolimus from a multilayered PLGA stent matrix. *Biomaterials*. 2006;27:5588–95.
- Luong-Van E, Grondahl L, Chua KN, Leong KW, Nurcombe V, Cool SM. Controlled release of heparin from poly(epsilon-caprolactone) electrospun fibers. *Biomaterials*. 2006;27:2042–50.
- Khan W, Farah S, Domb AJ. Drug eluting stents: developments and current status. *J Control Release*. 2012;161:703–12.
- Biondi M, Ungaro F, Quaglia F, Netti PA. Controlled drug delivery in tissue engineering. *Adv Drug Deliv Rev*. 2008;60:229–42.
- Kowalczyk T, Nowicka A, Elbaum D, Kowalewski TA. Electrospinning of bovine serum albumin. Optimization and the use for production of biosensors. *Biomacromolecules*. 2008;9:2087–90.
- Montero RB, Vial X, Nguyen DT, Farhand S, Reardon M, Pham SM, *et al*. bFGF-containing electrospun gelatin scaffolds with controlled nano-architectural features for directed angiogenesis. *Acta Biomater*. 2012;8:1778–91.
- Ekaputra AK, Prestwich GD, Cool SM, Huttmacher DW. The three-dimensional vascularization of growth factor-releasing hybrid scaffold of poly (epsilon-caprolactone)/collagen fibers and hyaluronic acid hydrogel. *Biomaterials*. 2011;32:8108–17.
- Hyung II RM, Kim JS, Konno T, Takai M, Ishihara K. Preparation of electrospun poly(L-lactide-co-caprolactone-co-glycolide)/phospholipid polymer/rapamycin blended fibers for vascular application. *Curr Appl Phys*. 2009;9:249–51.
- Okuda T, Tominaga K, Kidoaki S. Time-programmed dual release formulation by multilayered drug-loaded nanofiber meshes. *J Control Release*. 2010;143:258–64.
- Xie J, Wang CH. Electrospun micro- and nanofibers for sustained delivery of paclitaxel to treat C6 glioma *in vitro*. *Pharm Res*. 2006;23:1817–26.
- Cui W, Li X, Zhu X, Yu G, Zhou S, Weng J. Investigation of drug release and matrix degradation of electrospun poly(DL-lactide) fibers with paracetamol inoculation. *Biomacromolecules*. 2006;7:1623–9.
- Li M, Guo Y, Wei Y, MacDiarmid AG, Lelkes PI. Electrospinning polyaniline-contained gelatin nanofibers for tissue engineering applications. *Biomaterials*. 2006;27:2705–15.
- Li M, Mondrinos MJ, Chen X, Gandhi MR, Ko FK, Lelkes PI. Co-electrospun poly(lactide-co-glycolide), gelatin, and elastin blends for tissue engineering scaffolds. *J Biomed Mater Res A*. 2006;79:963–73.
- Uttayarat P, Perets A, Li M, Pimton P, Stachelek SJ, Alferiev I, *et al*. Micropatterning of three-dimensional electrospun polyurethane vascular grafts. *Acta Biomater*. 2010;6:4229–37.
- Crapo PM, Wang Y. Physiologic compliance in engineered small-diameter arterial constructs based on an elastomeric substrate. *Biomaterials*. 2010;31:1626–35.
- Han J, Lazarovici P, Pomerantz C, Chen X, Wei Y, Lelkes PI. Co-electrospun blends of PLGA, gelatin, and elastin as potential nonthrombogenic scaffolds for vascular tissue engineering. *Biomacromolecules*. 2011;12:399–408.
- Naseerali CP, Hari PR, Sreenivasan K. The release kinetics of drug eluting stents containing sirolimus as coated drug: role of release media. *J Chromatogr B Anal Technol Biomed Life Sci*. 2010;878:709–12.
- Okner R, Oron M, Tal N, Nyska A, Kumar N, Mandler D, *et al*. Electrocoating of stainless steel coronary stents for extended release of paclitaxel. *J Biomed Mater Res A*. 2009;88:427–36.

25. Uttayarat P, Chen M, Li M, Allen FD, Composto RJ, Lelkes PI. Microtopography and flow modulate the direction of endothelial cell migration. *Am J Physiol Heart Circ Physiol*. 2008;294:H1027–1035.
26. Mack MJ, Banning AP, Serruys PW, Morice MC, Tacymans Y, Van Nooten G, *et al*. Bypass *versus* drug-eluting stents at three years in SYNTAX patients with diabetes mellitus or metabolic syndrome. *Ann Thorac Surg*. 2011;92:2140–6.
27. Barner HB. Status of percutaneous coronary intervention and coronary artery bypass. *Eur J Cardio-Thorac*. 2006;30:419–24.
28. Mo XM, Xu CY, Kotaki M, Ramakrishna S. Electrospun P(LLA-CL) nanofiber: a biomimetic extracellular matrix for smooth muscle cell and endothelial cell proliferation. *Biomaterials*. 2004;25:1883–90.
29. Zong X, Kim K, Fang D, Ran S, Hsiao B, Chu B. Structure and process relationship of electrospun bioabsorbable nanofiber membranes. *Polymer*. 2002;43:4403–12.
30. He SW, Li SS, Hu ZM, Yu JR, Chen L, Zhu J. Effects of three parameters on the diameter of electrospun poly(ethylene oxide) nanofibers. *J Nanosci Nanotechnol*. 2011;11:1052–9.
31. Han J, Chen TX, Branford-White CJ, Zhu LM. Electrospun shikonin-loaded PCL/PTMC composite fiber mats with potential biomedical applications. *Int J Pharm*. 2009;382:215–21.
32. Desai K, Kit K, Li J, Zivanovic S. Morphological and surface properties of electrospun chitosan nanofibers. *Biomacromolecules*. 2008;9:1000–6.
33. Gandhi PJ, Murthy ZVP. Solubility and crystal size of sirolimus in different organic solvents. *J Chem Eng Data*. 2010;55:5050–4.
34. Tan EP, Ng SY, Lim CT. Tensile testing of a single ultrafine polymeric fiber. *Biomaterials*. 2005;26:1453–6.
35. Ferron GM, Jusko WJ. Species differences in sirolimus stability in humans, rabbits, and rats. *Drug Metab Dispos*. 1998;26:83–4.
36. Simamora P, Alvarez JM, Yalkowsky SH. Solubilization of rapamycin. *Int J Pharm*. 2001;213:25–9.
37. Verreck G, Chun I, Rosenblatt J, Peeters J, Dijk AV, Mensch J, *et al*. Incorporation of drugs in an amorphous state into electrospun nanofibers composed of a water-insoluble, nonbiodegradable polymer. *J Control Release*. 2003;92:349–60.
38. Yang Y, Li X, Cui W, Zhou S, Tan R, Wang C. Structural stability and release profiles of proteins from core-shell poly (DL-lactide) ultrafine fibers prepared by emulsion electrospinning. *J Biomed Mater Res A*. 2008;86:374–85.
39. Huatan H, Collett JH, Attwood D, Booth C. Preparation and characterization of poly(epsilon-caprolactone) polymer blends for the delivery of proteins. *Biomaterials*. 1995;16:1297–303.
40. Innocente F, Mandracchia D, Pektok E, Nottelet B, Tille JC, de Valence S, *et al*. Paclitaxel-eluting biodegradable synthetic vascular prostheses: a step toward reduction of neointima formation? *Circulation*. 2009;120(11 Suppl):S37–45.